JOURNAL OF GEOPHYSICAL RESEARCH: ATMOSPHERES, VOL. 118, 1563–1576, doi:10.1002/jgrd.50181, 2013

The contributions of chemistry and transport to low arctic ozone in March 2011 derived from Aura MLS observations

S. E. Strahan,[1] A. R. Douglass,[2] and P. A. Newman[2]

Received 22 March 2012; revised 8 January 2013; accepted 14 January 2013; published 14 February 2013.

[1] Stratospheric and total columns of Arctic O_3 (63–90°N) in late March 2011 averaged 320 and 349 DU, respectively, 50–100 DU lower than any of the previous 6 years. We use Aura Microwave Limb Sounder (MLS) O_3 observations to quantify the roles of chemistry and transport and find there are two major reasons for low O_3 in March 2011: heterogeneous chemical loss and a late final warming that delayed the resupply of O_3 until April. Daily vortex-averaged partial columns in the lowermost stratosphere ($p > 133$ hPa) and middle stratosphere ($p < 29$ hPa) are largely unaffected by local heterogeneous chemistry, according to model calculations. Very weak transport into the vortex between late January and late March contributes to the observed low ozone. The lower stratospheric (LS) column (133–29 hPa, ~370–550 K) is affected by both heterogeneous chemistry and transport. Because MLS N_2O data show strong isolation of the vortex, we estimate the contribution of vertical transport to LS O_3 using the descent of vortex N_2O profiles. Simulations with the Global Modeling Initiative (GMI) chemistry and transport model (CTM) with and without heterogeneous chemical reactions show 73 DU vortex averaged O_3 loss; the loss derived from MLS O_3 is 84 ± 12 DU. The GMI simulation reproduces the observed O_3 and N_2O with little error and demonstrates credible transport and chemistry. Without heterogeneous chemical loss, March 2011 vortex O_3 would have been at least 40 DU lower than climatology due to the late final warming that did not resupply O_3 until mid-April.

Citation: Strahan, S. E., A. R. Douglass, and P. A. Newman (2013), The contributions of chemistry and transport to low arctic ozone in March 2011 derived from Aura MLS observations, *J. Geophys. Res. Atmos.*, *118*, 1563–1576, doi:10.1002/jgrd.50181.

1. Introduction

[2] Very low Arctic mean (63–90°N) column O_3 was observed by the Ozone Monitoring Instrument (OMI) and the Microwave Limb Sounder (MLS) on the NASA Aura satellite in March 2011. Averaged over 20–26 March, OMI and MLS measured 349 DU (total column in Dobson units) and 320 DU (stratospheric column calculated from profiles), respectively. Figure 1 shows the OMI and MLS column ozone from 24 March 2011; both instruments show regions of less than 250 DU. The MLS Arctic mean O_3 in Figure 1c shows considerable interannual (IA) variability in late winter; however, the low columns found in 2011 (red) are in sharp contrast with the previous 6 years. MLS Arctic mean stratospheric column and OMI total column O_3 from 2005–2010 averaged 74 DU higher—394 DU and 423 DU, respectively—during this same one week period in late March.

[3] The 2011 Arctic vortex was unusual in its longevity and in the strength of its mixing barrier [*Manney et al.*, 2011]. Weak eddy heat flux in February allowed the vortex to stay strong, keeping lower stratospheric (LS) vortex temperatures at or below the threshold of chlorine activation until late March [*Hurwitz et al.*, 2011]. The persistence of such meteorological conditions for more than 3 months is typical of the Antarctic but has not previously been observed in the Arctic. Although recent cold Arctic springs, notably 1997, 2000, 2003, and 2005, had a March vortex with sufficiently low temperatures to produce daily March minimum O_3 columns as low as ~320 DU (averaged poleward of 63° equivalent latitude), they did not have a period of polar stratospheric cloud (PSC) formation that lasted more than 3 months [*WMO*, 2011]. The lengthy period of low temperatures in 2011 led to a much greater degree of denitrification and subsequent ozone loss than has been previously diagnosed in the Arctic [*Manney et al.*, 2011; *Sinnhuber et al.*, 2011].

[4] Winters with above average stratospheric wave activity have a warm, disturbed vortex, while winters with weak wave driving have a cold, long lasting vortex, with well-known impacts on Arctic March temperatures [*Newman et al.*, 2001] and column O_3 [*Chipperfield and Jones*, 1999; *Rex et al.*, 2004; *Tegtmeier et al.*, 2008]. Greater poleward and downward transport of ozone in warm

[1]Universities Space Research Association, Columbia, Maryland, USA.
[2]NASA Goddard Space Flight Center, Greenbelt, Maryland, USA.

Corresponding author: S. E. Strahan, NASA Goddard Space Flight Center, Code 614, Greenbelt, MD 20771, USA. (Susan.e.strahan@nasa.gov)

2169-897X/13/10.1002/jgrd.50181

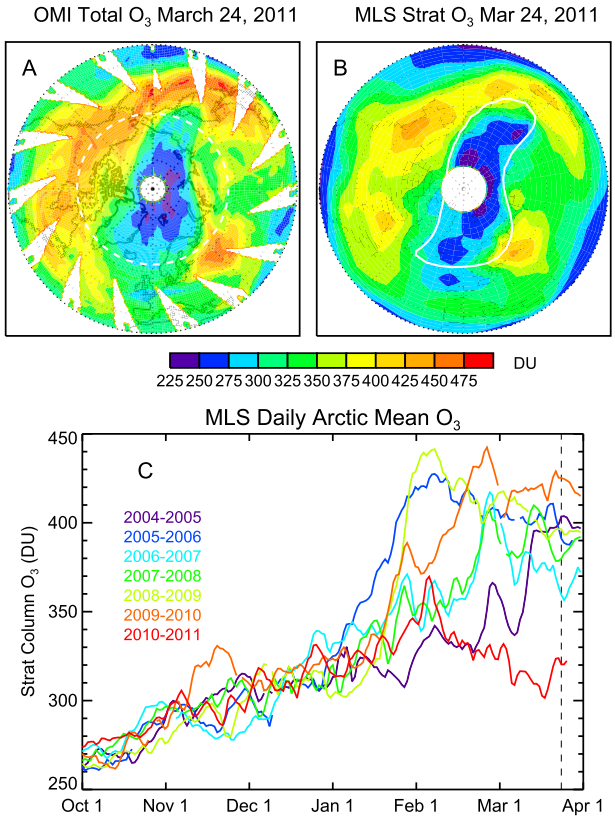

Figure 1. (a) OMI total column O_3 in the Arctic, 24 March 2011. The white dashed line is 63°N. (b) MLS stratospheric column O_3 on 24 March 2011. The white solid line shows the vortex edge (PV = 5 x 10^{-5} K m^2 kg^{-1} s^{-1}). The difference between Figures 1a and 1b is the tropospheric column, ~25–35 DU. (c) Daily MLS Arctic Mean (63°–88°N) stratospheric column O_3 time series from 1 October to 1 April for seven fall/winter seasons, 2004–2011. 24 March is indicated by the dashed line.

winters leads to higher levels of March ozone. The converse is true for cold winters. The relationship between dynamical variability and O_3 was demonstrated by *Randel et al.* [2002], who showed the link between changes in stratospheric wave driving (i.e., the Eliassen-Palm flux) and ozone transport to high latitudes in spring, concluding that hemispheric ozone trends were caused in part by the wave driving trends from 1979–2000. *Chipperfield and Jones* [1999] also observed this relationship and concluded that dynamical variability in the 1990s contributed more to IA variability in March Arctic O_3 than chemical loss. *Müller et al.* [2008] showed that the appearance of large dynamical variability of Arctic O_3 could be reduced by use of a dynamical coordinate, equivalent latitude, which helped to reveal the correlation between March Arctic O_3 and ozone loss.

[5] Cold winters can have lower March ozone due to increased frequency of PSCs and weaker wave-driven transport, but a delayed resupply of higher O_3 to the Arctic may also contribute if the final warming occurs in April. Herein lies one of the difficulties in quantifying chemical O_3 loss: Arctic March column O_3 has large IA variability, and its climatological mean may not be representative of any given year. This can be an especially large problem in years such as 1997 and 2011 which were cold enough to have significant chemical loss but did not have a final warming until April. The final warming, in which the weakened vortex edge allows isentropic mixing of midlatitude air into the vortex, can supply more than 40 DU O_3 to the Arctic.

[6] In this paper, we use Aura MLS O_3 and N_2O observations and the Global Modeling Initiative (GMI) chemistry and transport model (CTM) to quantify transport into the Arctic vortex in 2011 and calculate the heterogeneous chemical loss. We examine MLS Arctic O_3 behavior from October to March for the years 2004–2011 to characterize column O_3 variability. Analysis of vortex partial column O_3 above and below the levels of PSC occurrences demonstrates the effects of reduced transport in 2011 on those parts of the column. Analysis of MLS LS temperatures, and column O_3 shows there is little IA variability in transport inside the Arctic vortex before a warming occurs, allowing us to estimate the early winter LS column available for chemical loss in 2011. The descent of MLS N_2O profiles within a strongly isolated vortex provides a means to calculate the small effect of vertical transport on LS vortex O_3 in late winter. By quantifying the transport contributions to vortex O_3, we can calculate the chemical O_3 loss averaged over the vortex.

[7] In support of the observational analysis, the GMI CTM was integrated with Goddard Earth Observing System (GEOS) Modern-Era Retrospective Analysis for Research and Application (MERRA) meteorological fields in simulations with and without heterogeneous chemistry to quantify O_3 loss. MERRA is a NASA meteorological reanalysis for the satellite era using version 5 of the GEOS Data Assimilation System (GEOS-5) [*Rienecker et al.*, 2011]. Comparisons between simulated and observed Arctic N_2O verify accurate transport by the model throughout fall and winter. Further, the close agreement between simulated and observed O_3 and ClO indicates that both model transport and chemistry are realistic. The difference between vortex O_3 in the two simulations is within the observational uncertainty of the O_3 loss calculated from MLS data, demonstrating that the method applied to the 2011 MLS data provides an accurate estimate of O_3 loss.

2. MLS Observations and the GMI CTM

[8] This study uses Aura MLS v3.3 Level 2 profile measurements of temperature, O_3, N_2O, and ClO on pressure surfaces between October 2004 and March 2011 [*Livesey et al.*, 2011]. Due to an instrument anomaly, MLS did not make observations between March 27 and 18 April 2011. MLS v3.3 O_3 and temperature data are reported on a high vertical resolution grid with 12 pressures per decade; N_2O and ClO are reported on six pressure levels per decade. *Livesey et al.* [2011] report the 2σ accuracy of MLS v3.3 O_3 columns as 4%. For MLS N_2O observations, the 2σ accuracy in the lower stratosphere is reported as 14% [*Livesey et al.*, 2011]. Uncertainties in O_3 and ClO profile data are discussed in section 4.2. Aura OMI total column O_3 data are used to calculate 63–90°N averages. OMI is a UV/visible backscatter instrument that make measurements only in the sunlit globe, thus latitudes poleward of 70°N are not sampled until mid-February. The OMI column O_3 mean bias error is reported as less than 2% [*Anton et al.*, 2009].

[9] In this study, we calculate MLS columns using data poleward of 54°N, from 268 to 0.46 hPa, and examine them inside and outside the vortex during a 7 year period. The lowest MLS O_3 level used, 268 hPa, is generally near the tropopause inside the vortex but below the tropopause outside at high northern latitudes. *Nash et al.* [1996] showed that the colocation of the steepest potential vorticity (PV) gradient and the jet maximum on a potential temperature surface can be used to define the vortex edge. We find that PV = 5 (10^{-5} K m^2 kg^{-1} s^{-1}) on the 500 K surface is located in the region of steep gradients for all winters studied. We use daily PV fields from the GEOS-MERRA assimilation to determine whether an MLS observation is inside the Arctic vortex. The location of the PV-based edge varies with height, but only one edge definition may be used when evaluating column quantities. The PV = 5 (on 500 K) vortex edge definition used here is closely aligned with the location of large PV gradients in the lower stratosphere (400–550 K) and in the middle stratosphere (MS) (600–700 K). Ozone between 400 and 700 K represents roughly three quarters of the stratospheric column.

[10] The GMI CTM was integrated from 1 October 2010 to 30 April 2011 using GEOS-MERRA meteorological fields [*Rienecker et al.*, 2011] with 1° x 1.25° horizontal resolution and 72 vertical levels having ~1 km resolution between 300 and 10 hPa. Details of the GMI CTM including chemical mechanism can be found in *Strahan et al.* [2007] and *Duncan et al.* [2007]. The stratospheric chemical mechanism [*Douglass and Kawa*, 1999] and the polar stratospheric cloud parameterization [*Considine et al.*, 2000] used in GMI are the same as those used in the GEOS chemistry climate model (GEOSCCM). *The SPARC Chemistry Climate Model validation* activity [SPARC, 2010] determined that GEOSCCM produced Antarctic O_3 loss consistent with observations. In addition, radicals, reservoirs, and precursor species were found to be well represented. High horizontal resolution was chosen to reduce the area of polar cap averaging used by the advection scheme (by a factor of 4 compared to a 2° x 2.5° simulation). This improvement is crucial for the accurate representation of descent over the pole; see *Allen et al.* [2011] for an illustration of this effect. In a second GMI integration ("No Het"), the rates for heterogeneous reactions involving Cl and Br were set to zero, turning off processing by PSCs, binary and ternary solutions, and ice. The difference in O_3 fields between the "No Het" and the full chemistry ("Het") simulation is referred to as the PSC-driven loss. Gas phase O_3 loss reactions become important in the Arctic in late winter so it is important that they are included in both simulations. Their omission in "No Het" would result in O_3 being too high by late March.

3. Interannual Variability of Arctic Ozone

3.1. Variability Inside and Outside the Vortex

[11] Horizontal mixing at the edge of the polar vortex can be very weak; thus, polar transport processes and their variability affect vortex and nonvortex O_3 differently. Figure 2 shows daily vortex and nonvortex-averaged column O_3 from October through March, calculated using the daily location of PV = 5 on the 500 K surface to define the vortex edge. The vortex can be defined by this PV value by mid-November. The daily means are area weighted and use all MLS O_3 observations poleward of 54°N from 2004 to 2011. The 54°N lower latitude limit was chosen in order to include the vortex during most wave events when it is pushed well off the pole. The Arctic mean column depends on the means of the vortex and nonvortex columns as well as the fractional area of each region. Figure 2c shows the time series of vortex area as a percentage of the Arctic (54°–90°N).

[12] Figure 2 shows that column O_3 increases during fall and winter in all years both inside and outside the vortex; this is a well-understood consequence of poleward and downward transport of O_3 from its low-latitude source region by the Brewer–Dobson circulation [e.g., *Newman et al.*, 2001; *Randel et al.*, 2002]. Arctic columns outside the vortex have greater IA variability from mid-December through March, coincident with the period of greatest midlatitude eddy heat flux [*Randel et al.*, 2002]. Vortex O_3 variability for the years shown is quite low until late January; after this time, a major warming may cause a large, rapid increase in vortex O_3 by mixing with midlatitude air or by breakdown of the vortex (e.g., 2006, 2009, and

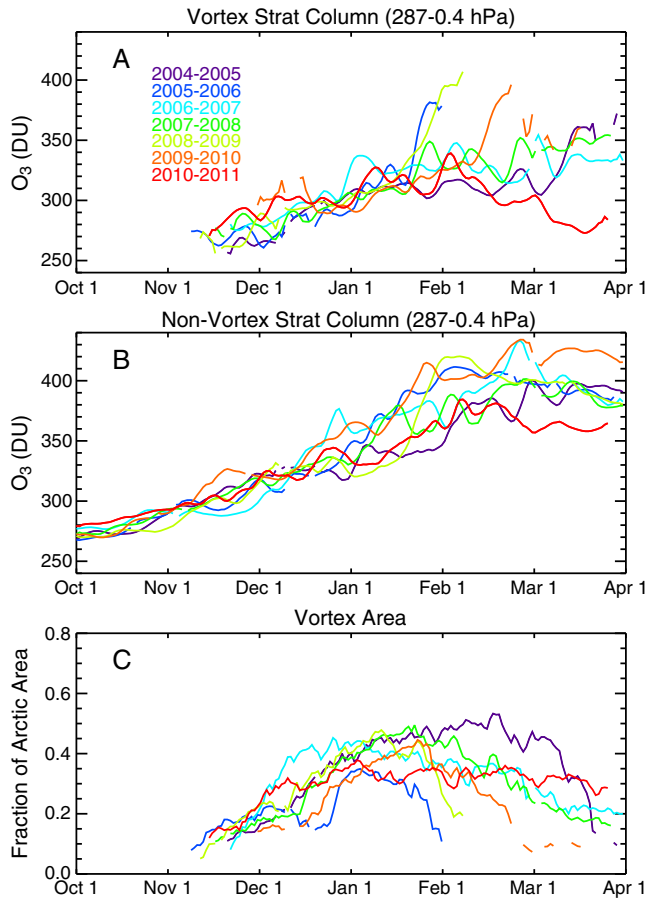

Figure 2. Daily MLS stratospheric column O_3 for 2004–2011. (a) Averaged inside the Arctic vortex, (b) averaged outside the vortex and poleward of 54°N. (c) The fraction of the area poleward of 54°N occupied by the Arctic vortex. The vortex is defined by areas with PV ≥ 5 on the 500 K surface. After a major warming, the vortex area may drop to zero.

2010) and replacement with midlatitude air. Variations in tropopause height also lead to daily variability in the lowermost stratosphere (LMS) and LS O_3 columns, about 1.6 DU/100 m change in tropopause height [*Steinbrecht et al.*, 1998]. The use of vortex mean quantities reduces this source of variability. Figure 2 shows that large contributions to Arctic mean column variability, as seen in Figure 1c, include vortex area, column amounts outside the vortex beginning in early winter, and vortex column amounts after mid-January. The very low stratospheric column outside the vortex in March 2011 is consistent with unusually weak wave driving (i.e., eddy heat flux) observed in February [*Hurwitz et al.*, 2011].

[13] The formation of the vortex in fall is governed by radiative processes at a time when seasonal wave activity is weak. Thus, the IA variability of vortex O_3 in fall is low because there is little IA variability in the radiative and photochemical processes controlling it [*Kawa et al.*, 2002]. Vortex temperatures reflect the low IA variability in early season wave transport. The solid color lines in Figure 3 show the daily means of vortex temperatures at 68 hPa for seven recent Arctic winters. The dashed (dotted) lines show the 10th and 90th (25th and 75th) percentiles of all daily observed vortex temperatures for 7 years. From October to about 20 January, the daily area-weighted means (colored lines) are usually within 2 K of the 7 year mean temperatures (black). MLS vortex temperatures between 146 and 21 hPa show similar low early season variability. In the absence of a large wave event such as a major warming, vortex temperatures in fall and early winter are similar each year, producing diabatic descent and radiatively driven downward transport of the O_3 column [*Kawa et al.*, 2002]. In addition, *Kawa et al.* [2002] report that vortex O_3 profiles in November have low IA variability; thus, the combination of low IA variability in both vortex O_3 profiles and descent rates leads to low IA variability in vortex column O_3. In late January, wave driving often increases and so do the ranges of vortex temperature, mean column O_3, and area (Figures 3, 2a, and 2c). Breaking planetary waves increase the strength of the circulation and drive polar stratospheric temperatures away from radiative equilibrium [*Newman et al.*, 2001]. The warmer polar temperatures result in diabatic descent; the descent of potential temperature surfaces appears as an increase in temperature on a constant pressure surface, e.g., 2005–2010 in Figure 3. The strengthened circulation also increases the poleward and downward transport of O_3, and the concomitant increase in temperature reduces PSC formation. Conversely, winters with reduced wave driving have reduced poleward downward transport of O_3, reduced temperatures, and greater O_3 losses from PSCs. The very low temperatures observed in February and March 2011 (red) combined with the results of *Hurwitz et al.* [2011] demonstrating unusually low heat flux strongly suggest that vortex descent in 2011 was much weaker than usual. The 2011 MLS vortex late winter temperatures from 121 to 32 hPa are also nearly constant, indicating weak descent at those levels as well.

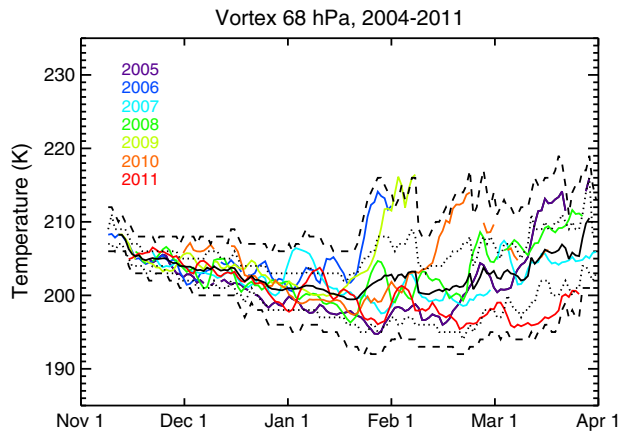

Figure 3. Daily average MLS 68 hPa temperatures for seven fall/winter seasons (colored lines) inside the Arctic vortex. Heavy black line is the average of 7 years of daily averages. Dotted lines are the 25th and 75th percentiles of all daily temperatures observed for all years. Dashed lines show the 10th and 90th percentiles.

3.2. Partial Stratospheric Columns Inside the Vortex

[14] Arctic vortex column O_3 after mid-January shows large variability due to the IA variability of planetary wave driven transport, i.e., the strength of the residual circulation transporting O_3 and the strength of the vortex edge as a mixing barrier. The differences in wave driving also directly affect vortex temperature [*Newman et al.*, 2001] and hence the degree of PSC-driven O_3 loss. To separate the effects of chemistry and transport in 2011, we examine time series of partial columns. PSC-forming temperatures in the Arctic vortex typically occur on potential temperature surfaces ranging from 370 to 550 K [*Rex et al.*, 2006; *Tegtmeier et al.*, 2008], approximately 120–30 hPa. Temperature conditions for PSC formation occur infrequently in the LMS ($p > 120$ hPa) or the MS ($p < 30$ hPa) and may not occur during sunlit conditions. Analysis of partial ozone columns in the LMS and MS allows us to assess how transport affects much of the stratospheric column during fall and winter without the complication of heterogeneous chemistry. We compute partial columns based on the pressure difference between the top and bottom edges of a box where the MLS-reported pressure level is the midpoint. The top and bottom edge pressures are calculated as the midpoint in log-pressure between adjacent levels. The LS column where PSCs may form spans 133–29 hPa, which includes all midpoint pressure levels 121–32 hPa. It is approximately coincident with the column from 370–550 K, which encompasses the range of potential temperatures used in other studies of Arctic O_3 depletion [e.g., *Rex et al.*, 2006; *Tegtmeier et al.*, 2008; *Manney et al.*, 2011]. Heterogeneous chemical losses are likely to take place only in this vortex partial column. The possibility of O_3 loss in the LMS and MS will be addressed later with the GMI CTM.

[15] Figure 4 shows the time series for MLS LMS (287–133 hPa) and MS (29–0.4 hPa) column O_3 inside the vortex for seven Arctic winters. Fall and early winter show nearly the same, gradually increasing column amounts in all years, consistent with low stratospheric column variability shown in Figure 2a and the radiative control discussed in section 3.1. After mid-January 2005–2010, the LMS and MS vortex O_3 columns, which have negligible local heterogeneous chemical loss, show either continued

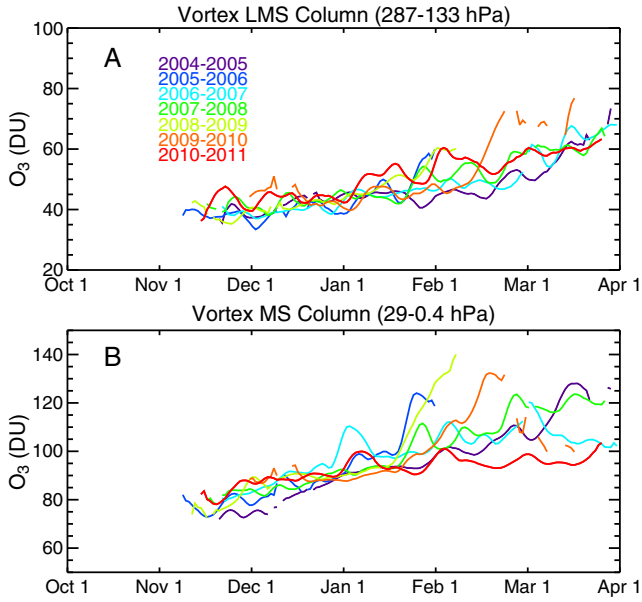

Figure 4. Daily MLS partial column O_3 averaged inside the vortex for seven fall and winter seasons. (a) The lowermost stratosphere (LMS) column, 287–133 hPa. (b) The middle/upper stratosphere (MS) column, 29–0.4 hPa.

gradual increase or a sudden large increase due to a major midwinter warming (2006, 2009, and 2010). In years with a major warming, the vortex is destroyed but reforms before the end of March.

[16] The LMS and MS O_3 columns in February and March 2011 show little increase. The MS partial column observed in late March is essentially unchanged from late January. The LMS column shows a small increase that is less than the other years. The lack of increase is consistent with LMS and MS temperatures that hold steady during this period (similar to LS temperatures shown in Figure 3), consistent with the extremely weak heat flux that is likely to limit diabatic descent. PV gradients show that the stratospheric vortex remains strong down to ~350 K, restricting horizontal transport across the vortex edge in the MS and the upper levels of the LMS. The Arctic tropopause is often near the bottom edge of the lowest MLS O_3 level (~287 hPa) where there is no meridional transport barrier, but the contribution to the LMS column is small here. The sum of these two partial columns in late winter 2011 is 25 DU lower than the average of the previous 6 years, highlighting the exceptionally weak transport. These results are consistent with the dynamical analysis of *Hurwitz et al.* [2011] that found that unusually weak wave driving led to an especially cold and isolated vortex that persisted until April.

[17] Ozone "mini-holes" are caused by a high tropopause, which lifts the O_3 column to lower pressures thus reducing the column [see, for example, *Hood et al.*, 2001]. Lifting produces adiabatic cooling, resulting in the observed correlation between column O_3 and temperature. *Manney et al.* [2011, supplement] showed the relationship between O_3 and tropopause height using observations from several cold Arctic winters. Other than brief periods in February 2011, the February and March 2011 vortex tropopause heights were not high compared to other years. We also find that vortex tropopause heights deviated little from the 2004–2011 mean (not shown) and conclude that tropopause height had no more than a transient dynamical effect on column O_3 values.

[18] Figure 5 shows GMI LMS and MS vortex-averaged column time series from the Het and No Het runs along with the MLS vortex averaged data from Figure 4. GMI vortex partial columns are calculated using the same methods applied to the MLS data and GMI partial column pressure boundaries are nearly the same as MLS. Figure 5 demonstrates three important results. First, the GMI Het simulation (red) matches the MLS time series (blue) to within a few DU at all times from November to March; the RMS differences are less than the 4% MLS column uncertainty. Because chemical processes are negligible, this shows the accuracy of simulated transport in the LMS and MS. Second, the GMI No Het LMS and MS time series support the results of the MLS analysis described above by showing almost no increase in vortex O_3 from late January to late March. Third, the GMI Het/No Het simulations confirm that heterogeneous chemical loss is negligible above or below the LS column. There is less than 1 DU O_3 loss in the MS partial column and less than 3 DU difference in the LMS column. In the first week of February, GMI Het shows a small enhancement of ClO near 26 hPa and a ~0.5 DU difference between No Het and Het appears at this time; no other periods of loss are found. A small enhancement of ClO in the LMS is found only in the first half of February, and by 15 February, the No Het-Het difference in the LMS vortex is about 0.5 DU. Between 15 February and 26 March, the No Het-Het LMS difference increases to 3 DU, but the model ClO is negligible, suggesting that in situ loss is not occurring. Rather, the likely cause is the descent of O_3-depleted vortex air into LMS column of the Het simulation. The GMI simulations establish that the analysis method applied to the MLS data correctly separates the stratospheric column into regions with and without heterogeneous chemistry.

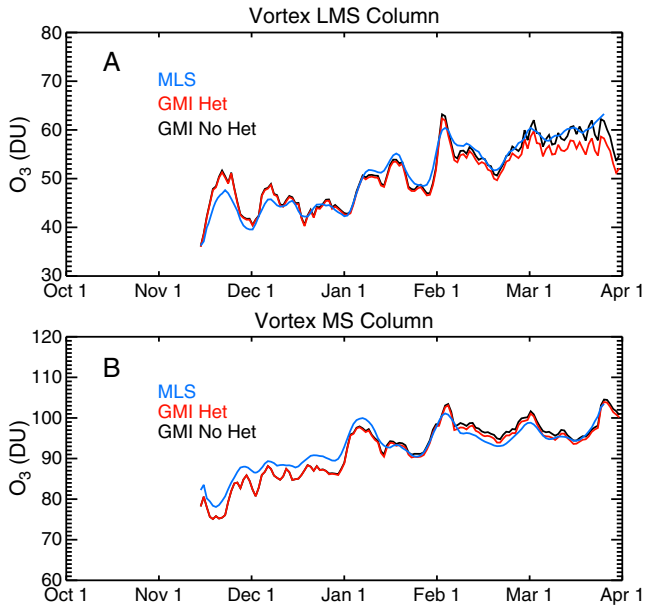

Figure 5. Daily MLS, GMI Het, and GMI No Het (a) lowermost stratosphere and (b) middle stratosphere partial column O_3 averaged inside the vortex for 2010–2011.

4. Separating the Effects of Transport and Chemistry in the LS Vortex O_3 Column

4.1. From Fall Through Late January

[19] Figure 6 shows MLS LS vortex column O_3 for 2004–2011. Before February, low IA variability of the O_3 columns is observed because transport is primarily radiatively controlled at high latitudes in fall and early winter (i.e., through diabatic descent) and gas phase chemistry is insignificant. For all years shown, the maximum LS vortex O_3 column in mid to late January is ~170–185 DU. After mid-January, vortex O_3 may increase due a sudden warming (e.g., 2006, 2009, and 2010), in which O_3-rich midlatitude air mixes into the vortex, or it may decrease due to chemical losses (e.g., 2005, 2007, 2008, and 2011). The late January O_3 maximum is reached before the onset of significant chemical loss. Notice that the LS vortex columns in early December 2010 (red) were near the top of the data envelope, while by late January 2011, they were on the low side. Given that PSCs and high ClO were observed in December 2010 and January 2011 [*Manney et al.*, 2011], it is probable that the change in the 2010–2011 O_3 from the high to the low side of the 7 years is due to early season chemical loss. Indeed, the difference between GMI Het and No Het LS vortex on 1 February is 13 DU. This estimate of early winter loss agrees with *Balis et al.* [2011], who also obtained a 13 DU vortex-averaged loss in January 2011 using a chemical transport model (CTM) integrated with forecast meteorological fields.

4.2. From Late January Through Late March

[20] Figure 4 showed that the absence of late winter O_3 transport in the middle and LMS distinguishes 2011 from the other years and suggests that transport of O_3 into the LS vortex column is likely to be small. We quantify transport into the LS vortex during late winter by examining the changes in MLS N_2O vortex profiles. The key requirement in this analysis is that the vortex air be well-separated from midlatitudes so that the tracer-tracer correlation inside the vortex, or in this case the vortex N_2O profile, is isolated and unaffected by mixing across the vortex edge [*Müller et al.*, 2005]. This method uses the same principle employed by tracer-tracer correlation analyses to quantify O_3 loss within the vortex [e.g., *Müller et al.*, 1996; *Tilmes et al.*, 2003]. Separation of vortex from midlatitude air ensures that tracer-tracer correlations inside the vortex are not affected by mixing. Figure 7a shows the descent of MLS N_2O vortex average profiles on isentropic surfaces from early February (29 January–4 February average) to late March (20–26 March average); the 1σ uncertainties are shown by the dotted lines. The Arctic LS vortex maintained strong PV gradients at the edge throughout this time, and the mean vortex N_2O profile did not increase at any level, indicating that meridional transport of midlatitude air into the vortex (higher N_2O) was insignificant.

[21] The profile differences in the LS (400–550 K, or ~100–32 hPa) indicate net diabatic descent of 15 K (±8 K) over the 50 day period, or ~0.3 K potential temperature/

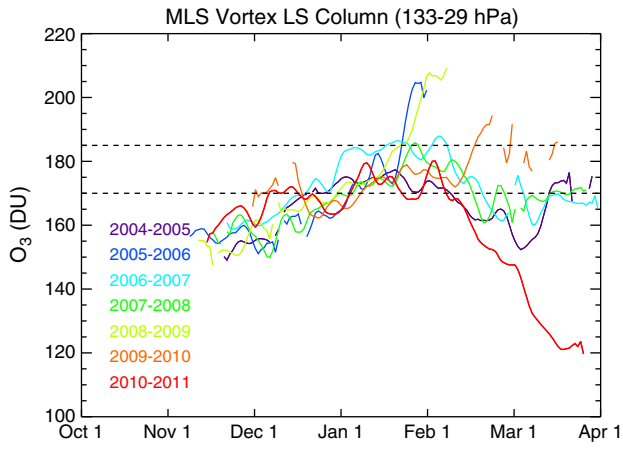

Figure 6. Daily MLS lower stratosphere vortex column O_3, 133–29 hPa (~370–550 K). The dashed lines show the approximate range of LS column amounts observed in mid-late January for all years, before major warmings (2006 and 2009).

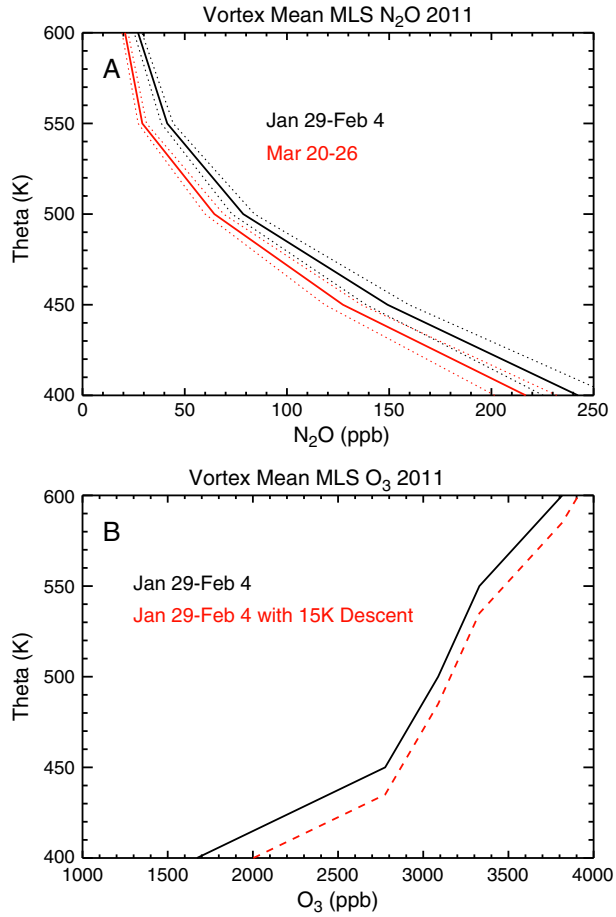

Figure 7. (a) Vortex-averaged N_2O profiles on isentropic (theta) surfaces 1 February (29 January—4 February average, black) and 23 March (20–26 March average, red). The dotted lines show the 1σ measurement uncertainty in the profiles. The N_2O profile descends 15 K in the lower stratosphere (400–550 K) during this period. (b) Vortex-averaged O_3 profile near 1 February (black) and the same profile shifted downward by 15 K to estimate the effect of descent on O_3 (red). These changes produce an estimated LS O_3 column increase of 14 DU, not including the effects of photochemical loss.

day. This small descent rate is consistent with the nearly constant temperature in the LS vortex shown in Figure 3. Note that the 15 K descent loses significance at the 2σ level below 450 K. In this regard, the 2011 Arctic vortex is much like the Antarctic. Late winter Antarctic LS vortex descent rates calculated by *Rosenfield et al.* [1994] are very similar to those calculated here for the 2011 Arctic, but are much smaller than those calculated in the same study for the Arctic (1988–1989 and 1991–1992). Figure 7b shows the effect of 15 K descent of the 1 February vortex O_3 profile, which increases the LS column by 14 DU. GMI diagnostics show that gas phase O_3 loss of ~4 DU (due to $NO_2 + O$) occurs in the Arctic during March above 550 K, reducing the net effect of transport (descent) on O_3 to 10 DU (2 DU in both the LS and MS columns). MLS N_2O cannot be used to estimate transport effects on the columns above or below the LS because N_2O is not retrieved in the LMS and MS vertical gradients are nearly zero.

[22] The insignificance of horizontal transport into the LS vortex is clearly shown by the contoured probability distribution functions (PDFs) of MLS LS N_2O in Figure 8. By early December, each PDF shows a distinct bimodal pattern indicating the separation of vortex and midlatitude air. The dashed black line marks 1 February. The purple and white regions indicate a near total lack of observations with mixing ratios intermediate between the vortex and midlatitude values (yellow/green bands) for all days between late January and late March. These PDFs confirm that the LS vortex was strongly isolated from midlatitudes and supports the use N_2O profile descent to estimate descent of the O_3 profile and its late winter contribution to the LS vortex column. N_2O PDFs on the 700 K and 800 K surfaces (not shown) also show strong isolation.

[23] The lower panels of Figure 8 show contoured PDFs from the GMI Het simulation on the same levels as MLS. The GMI PDFs closely match the MLS PDFs for all important features, such as the most probable values inside and outside the vortex and the lack of intermediate N_2O values (white and purple areas), demonstrating the realism of the simulated horizontal and vertical transport. There is a slight difference in descent of vortex air between 500 and 600 K between 1 February and late March. MLS N_2O's most probable values inside the vortex show weak descent occurring in February, while the model shows almost none. The weaker descent in the model is consistent with the smaller estimated increase in the LS vortex O_3 column during late winter in the No Het simulation, discussed in section 4.3. This leads to an underestimate of 7–10 DU O_3 loss for the GMI analysis.

[24] Realistic simulation of vortex O_3 during late winter requires that both transport and chemistry are accurate. Figure 9 compares GMI Het (black) and MLS (red) O_3 profiles at 80°N at the beginning and near the end of the period of large O_3 loss. All profiles shown are either inside the vortex or near the vortex edge. The MLS O_3 single profile precision is ~30–100 ppb over the altitude range shown, so most of the variability is geophysical. The zonal means for the model and observations, along with the MLS 2σ accuracy

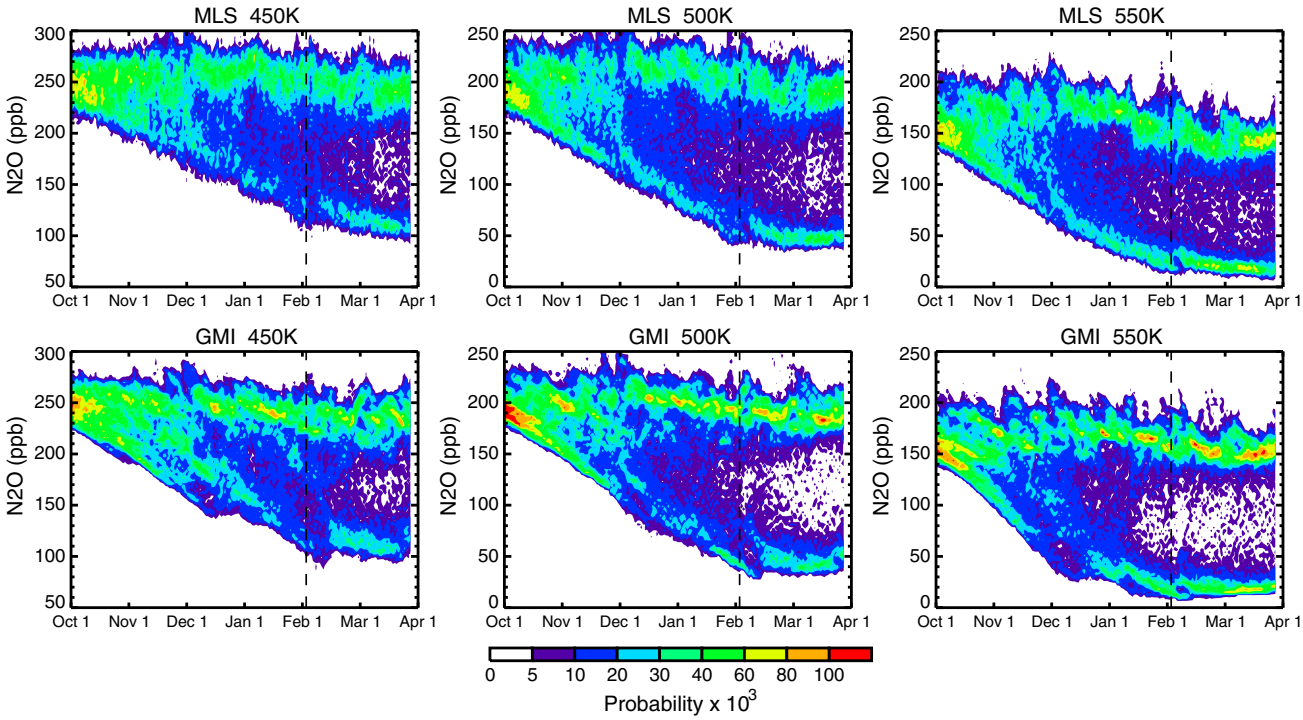

Figure 8. Contoured daily probability distribution functions (PDFs) of MLS and GMI N_2O 56–82°N on three isentropic surfaces in the lower stratosphere. The two distinct branches (December–April) indicate the isolation of the Arctic vortex. White and purple indicate there are almost no observations of a given mixing ratio, green/yellow/red indicate frequent observation of a given mixing ratio. The low N_2O branch represents vortex air. The mixing ratio of that branch decreases rapidly from October to February (descent) but very slightly during February and March.

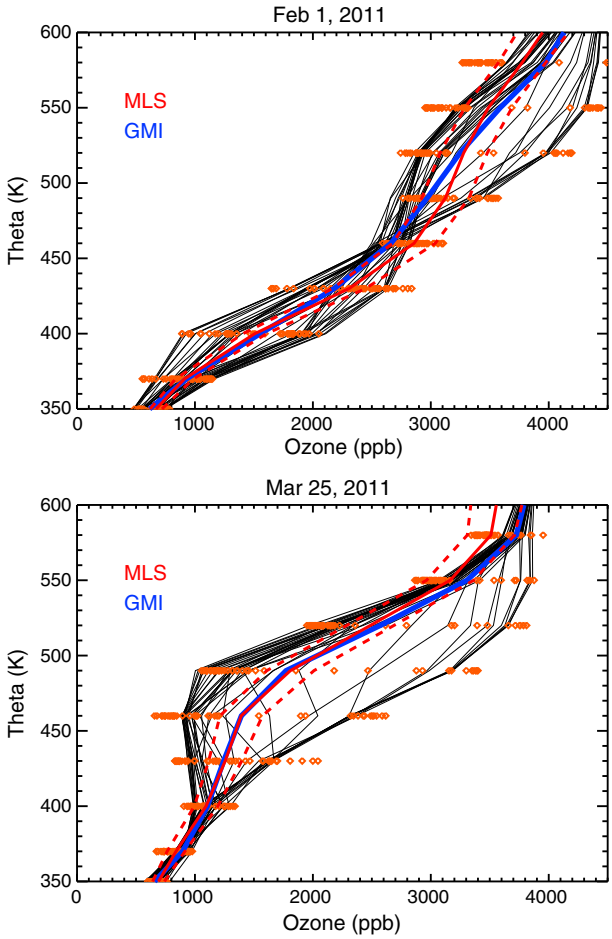

Figure 9. Forty MLS (red diamonds) and GMI (black lines) O_3 profiles on isentropic (theta) surfaces at 80°N, inside and at the edge of the vortex. The thick blue line is the model zonal mean. The thick red line is the MLS zonal mean and its 2σ uncertainty (dashed).

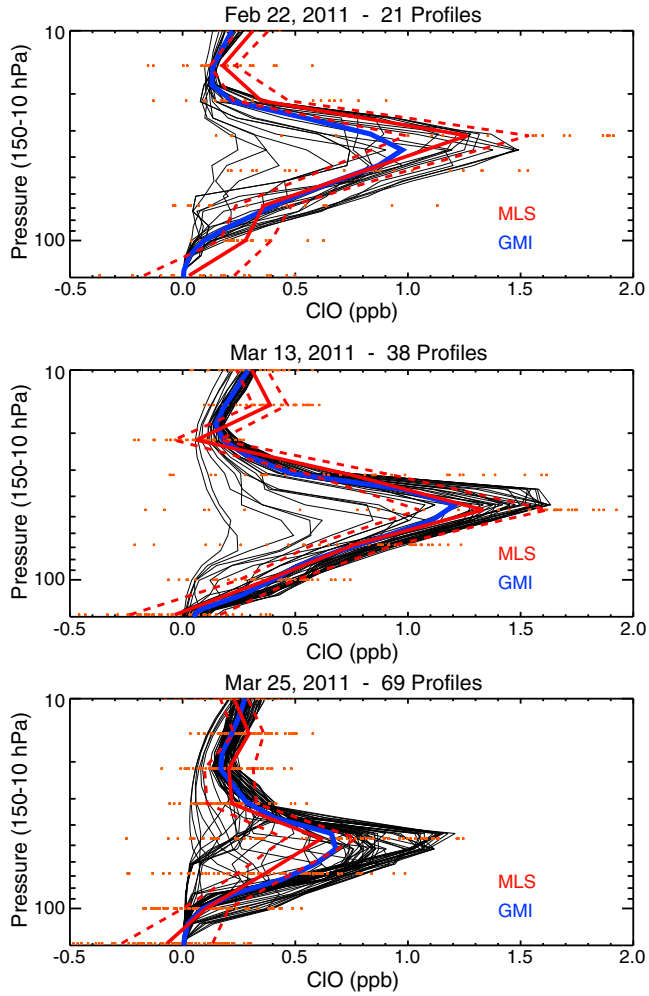

Figure 10. Midday MLS (red dots) and GMI (black lines) ClO profiles inside the vortex. The number of profiles meeting the comparison criteria increases toward spring (see text). The model mean profile is shown in blue; the thick red line is the MLS mean ClO profile. MLS ClO data are biased corrected according to http://mls.jpl.nasa.gov/data/MLS_v3-3_ClO_BiasCorrection.txt. The ClO 2σ uncertainties (red dashed) are calculated using the bias and scaling uncertainties given in Table 3.5.1 of the Aura MLS data quality document [*Livesey et al.*, 2011].

uncertainty (red dashed), are shown by the thick lines. This figure demonstrates that the simulation captures the mean high latitude O_3 profile very well both before and after large O_3 loss, and also the observed variability at each level in the lower stratosphere.

[25] Chlorine is responsible for the chemical changes in vortex O_3 during late winter. Figure 10 compares GMI and MLS ClO vortex profiles during the period of large O_3 loss. All observations are made at roughly 1:30 pm local time due to Aura's orbit, but model instantaneous output is only available at 12Z daily. Because of the large diurnal cycle in ClO, only model 12Z profiles inside the vortex that are within ~2 h of 1:30 pm local time can sensibly be compared. ClO vortex profiles with a solar zenith angle of less than 88°meeting these criteria are shown for three dates during late winter. MLS ClO single profile precision for pressures 147–31 hPa is ±0.1–0.3 ppb, but the overall uncertainty for a single profile can be much larger due to bias (±0.05 to ±0.2 ppb) and scaling uncertainties (±15 to ±40%) [*Livesey et al.*, 2011]. The MLS bias-corrected individual profiles in Figure 10 (red dots) reflect the large measurement uncertainty as well as geophysical variability. Averaging the MLS ClO profiles improves the precision and reduces the overall uncertainty, allowing a meaningful comparison with the model. The mean of each day's MLS vortex profiles that meet the model comparison criteria is shown in red along with 2σ uncertainty (red dashed). The simulated mean vortex profiles (thick blue) agree well with the MLS means and are almost always within the MLS 2σ uncertainty. Individual model profiles are shown with thin black lines.

4.3. Calculation of Ozone Loss From MLS Observations and the GMI Model

[26] Figure 11a shows that the evolution of the GMI Het LS vortex-averaged O_3 column and MLS column agrees to within ~10 DU or less (<7%) throughout the winter. The previous section demonstrated the physical basis for this good agreement by comparing simulated N_2O, O_3, and ClO with MLS observations to substantiate the credibility of

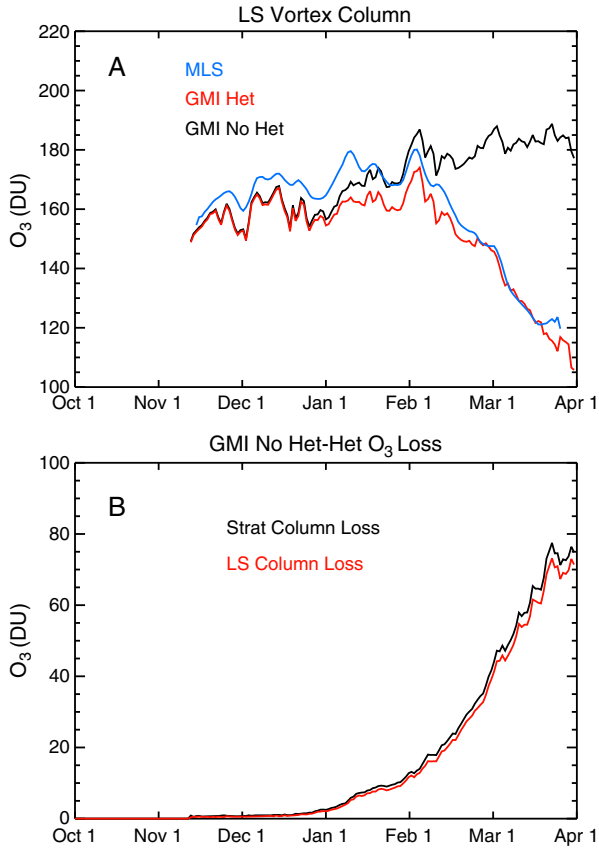

Figure 11. (a) Daily MLS, GMI Het, and GMI No Het lower stratospheric partial column O_3 (133–29 hPa) averaged inside the vortex for 2010–2011. (b) Cumulative O_3 loss inside the Arctic vortex due to heterogeneous chemical reactions determined by the difference between GMI No Het and Het total and lower stratospheric column O_3.

both the transport and chemistry of the GMI model. The black line in Figure 11a shows LS vortex column O_3 from the No Het simulation; the difference between the LS and stratospheric vortex columns for No Het and Het are shown in Figure 11b. This figure shows that the GMI model produces more than 70 DU O_3 loss by late March, with all but 4 DU of the loss occurring in the LS column.

[27] Figure 12 shows area-weighted PDFs for MLS, Het, and No Het vortex O_3 columns in middle and late winter to demonstrate how well the analysis separates the effects of the chemistry and transport. The top panels show that the means and distributions of the MLS stratospheric and LS vortex columns experience large and similar changes during late winter. The MLS LMS and MS partial column means and distributions show very little change, illustrating the near total lack of transport (vertical or horizontal). The change in the total stratospheric column in late winter corresponds almost entirely due to the change in the LS column.

[28] The GMI Het results in the middle row of Figure 12 show that the means and distributions of each partial column, both in middle and late winter, closely match MLS PDFs. These column results, combined with the excellent representation of GMI vortex profile N_2O, O_3, and ClO shown in Figures 8–10, further substantiate the credibility of chemistry and transport in the GMI simulation. The bottom row shows the PDFs for the GMI No Het run. The comparison with the GMI Het run reveals several important aspects of chemistry and transport during late winter. First, the No Het stratospheric vortex column increases only by about 5 DU over this 2 month period indicating extreme isolation and weak descent in the 2011 Arctic vortex. Note too that the shape of the distribution is virtually unchanged over this period. The No Het partial column PDFs individually show transport changes of +4, +3, and −1 DU for the LMS, LS, and MS, confirming the near total lack of transport in the vortex in the MS and below. Second, the differences between the PDFs in the middle row (Het) and the bottom row (No Het) illustrate the effects of PSC-driven chemical loss. (Chemical loss differences are also shown by the time series in Figures 5a and 5b and Figure 11a.) In the MS, the difference between the vortex columns reaches 0.6 DU around 1 February, but the late winter loss is only 0.4 DU. In the LMS, we find a difference in the Het/No Het vortex columns of 0.4 DU by 1 February, with an additional 0.5 loss by 20 February. We attribute the remainder of the ~2 DU difference in the LMS PDFs to the descent of O_3-depleted air in the Het run. In the LMS and MS in late winter, we find about 1 DU O_3 loss due to PSCs, suggesting that in the MLS analysis we are neglecting 1 DU O_3 loss in these partial columns in late winter. Almost all late winter loss, 57 DU, is confined to the LS column. Adding the LS late winter loss, the small losses in the LMS and MS (1 DU), the descent of O_3-depleted LS air into the LMS (~2 DU), and the early winter column loss (13 DU) bring the seasonal O_3 loss calculated by the GMI model to 73 DU. The GMI Het/No Het transport and chemistry results are summarized in Table 1.

[29] Table 2 summarizes the effects of transport and chemistry for the winter of 2010–2011 derived from MLS O_3 and N_2O. The MLS LMS and MS PDFs in the top row of Figure 12 show a 3.3 DU increase and a 1.5 DU decrease. For these columns, based on the GMI calculation, we estimate a combined PSC-driven loss of 1 DU after 1 February. Note also that we include a 4 DU gas phase chemical loss term, based on GMI chemical diagnostics. To estimate the heterogeneous chemical loss in the LS, we take the difference in vortex columns between late March and late January and add to that the contribution of O_3 that descended into the LS during this period as determined from descent of MLS N_2O profiles (Figure 7). This results in a 68 DU loss in the LS vortex. To estimate the loss for the stratospheric column averaged over the vortex for the entire season (fall and winter), we also include the small loss in the LMS and MS after 1 February (1 DU), descent of O_3-depleted LS air into the LMS (2 DU), and the loss of 13 DU for the entire column that occurs before 1 February, calculated by GMI. The full season loss derived primarily from the MLS observations is 84 DU with 12 DU 1σ uncertainty.

[30] The full season loss determined by the difference between the GMI No Het and Het runs is 73 DU. Although this value is within the 1σ uncertainty of the MLS result, we can explain the smaller model estimate by the weaker-than-observed descent in the model LS vortex during late winter. While the MLS N_2O profiles in Figure 7 descended by ~15 K (±8 K), the GMI N_2O vortex profiles (not shown) indicated only a few degrees potential temperature descent. (The lack of GMI descent can be seen in Figure 8. The

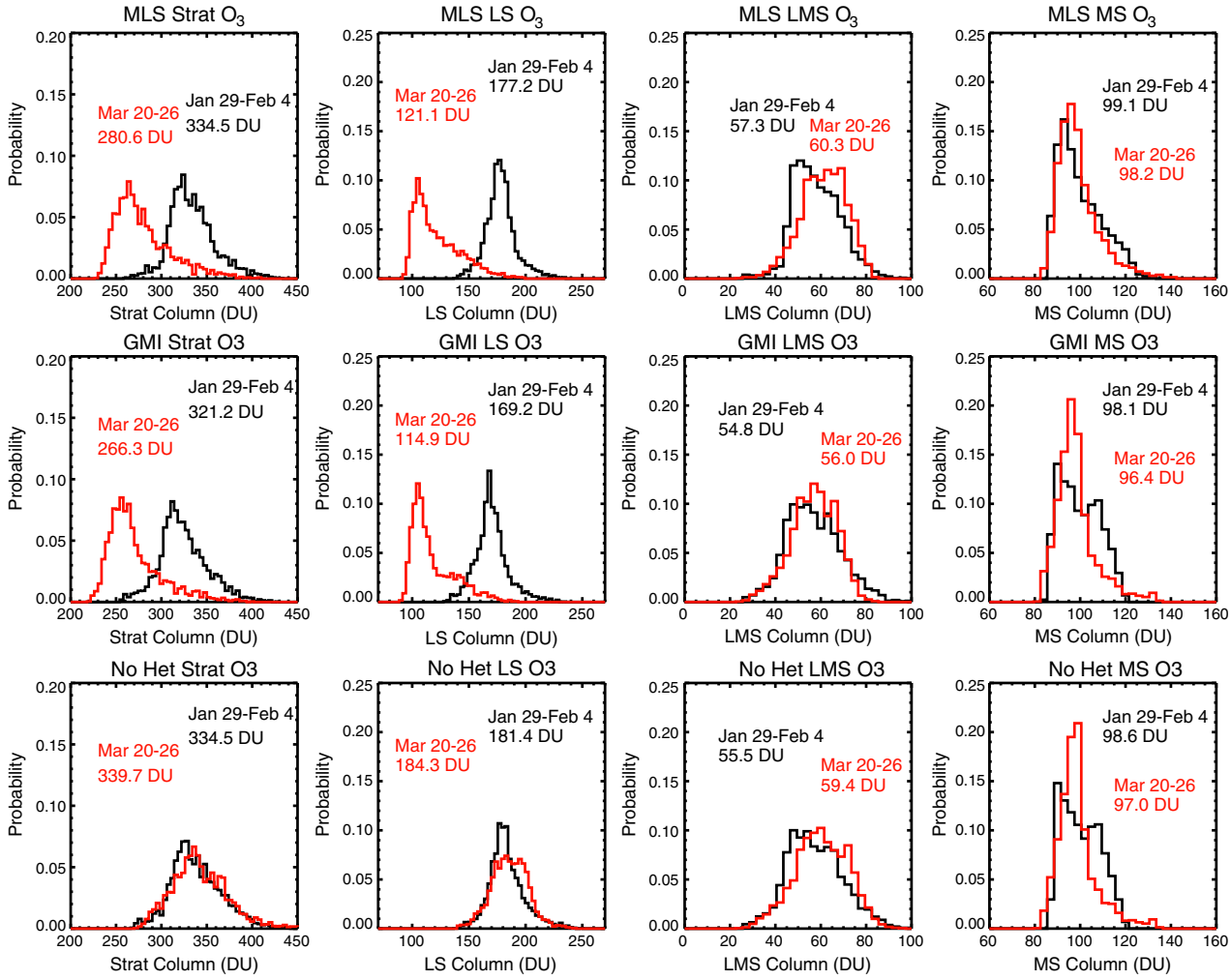

Figure 12. Top row: Comparison of PDFs of MLS vortex column O_3 at the end of January (29 January–4 February 2011, black) with MLS vortex columns, after the period of large chemical loss (20–26 March, red). The stratospheric and lower stratospheric columns show nearly the same change. The LMS and MS columns show very little change in their means or distributions. Middle row: Same as top row except for GMI Het simulation. Bottom row: Same as top row except for GMI No Het simulation.

Table 1. GMI Het and No Het Vortex Partial Column O_3: Late Winter Transport and Chemistry[a]

GMI No Het (DU)	1 Feb	23 Mar	Late Winter Transport[+]	Het Chemical Loss
LMS	55.5	59.4	3.9	--
LS	181.4	184.3	2.9	--
MS	98.6	97.0	−1.6	--
Strat	334.5	339.7	5.2	--
GMI Het (DU)				
LMS	54.8	56.0	3.9	0.5 + 2*
LS	169.2	114.9	2.9	57.2
MS	98.1	96.4	−1.6	0.4
Strat	321.2	266.3	5	60
Strat (Early winter)				13
Strat (season)				73

[a]Quantities are in Dobson units and are an average over 7 days, ±3 days of the date shown.

*~0.5 DU estimated in situ LMS chemical loss; ~2 DU is loss transported into LMS from the LS during this period.

[+]Includes gas phase losses.

vortex branch of the GMI N_2O PDF is nearly constant after 1 February.) An additional model descent of ~10 K would transport ~8 DU more O_3 to the LS column. Given the strong chlorine activation in the model during this season, the additional O_3 transported to the LS column would be largely destroyed, bringing the calculated loss up to 79–81 DU averaged over the vortex.

[31] Figure 13 shows stratospheric column O_3 for MLS and GMI Het for dates in January and March. Excellent agreement between the model and observations is found before and after the period of large PSC-driven losses. The lower left panel shows that the percentage difference between observed and simulated vortex mean column O_3 is always between 0 and −4%; the RMS error, 2.6%, is less than the MLS column O_3 2σ uncertainty (dashed lines). The total heterogeneous O_3 loss on 23 March is shown at the bottom right (GMI No Het-Het). About half the vortex shows losses of greater than 70 DU (yellow and orange).

[32] In the absence of heterogeneous chemical loss, the stratospheric vortex column mean in late March 2011 would

Table 2. MLS Vortex Partial Column O_3: Late Winter Transport and Chemistry[a]

MLS (1σ unc)	1 Feb	23 Mar	Gas Phase Loss[+]	Estimated Late winter Transport[¥]	Het Chemical Loss (Col 1-Col 2)+ (Col 4-Col 3)
LMS	57.3 (1.2)	60.3 (1.2)	0	3.3 (1.7)	~0.5 + 2*
LS	177.2 (3.6)	121.1 (2.4)	2	14 (7)	68.1
MS	99.1 (2.0)	98.2 (2.0)	2	1.5 (2)	~0.4
Strat (Late Winter)	334 (6.7)	280 (5.6)	4	19 (7)	71* (12)
Strat (Early Winter)					13 (from GMI)
Strat Vortex (season)					84 (12)

[a]Quantities are in Dobson units and are an average over 7 days, ± 3 days of the date shown.
[+]A total of 4 DU (LS+MS) gas phase column loss was calculated by the GMI model.
[¥]For the LMS and MS, the transport is inferred from the observed change in MLS vortex mean and the GMI calculated Het loss. For the LS, the transport was derived from the N_2O profile change (Figure 7).
*Estimated loss based on GMI Het calculation and on GMI-deduced transport of O_3-depleted air from the LS to the LMS (see Table 1).

have been 365 DU (84 DU estimated chemical loss + 281 DU observed by MLS). Four of the previous six years no longer had a vortex in late March, and their Arctic mean stratospheric columns ranged from 395 to 425 DU (Figure 1). The years that maintained a late March vortex, 2007 and 2008, had vortex-averaged O_3 of 335–355 DU and were estimated to have 80 DU or more PSC-driven losses [*WMO*, 2011], bringing their pre-loss columns to more than 400 DU. In the absence of chemistry, all six recent years would have late March Arctic or vortex mean column O_3 that was at least 30 DU higher than 2011. The key difference between 2011 and the previous 6 years is the lack of any significant late winter wave activity, including a final warming, before April 2011. The unusually weak wave activity and associated lack of transport have been documented by *Hurwitz et al*. [2011].

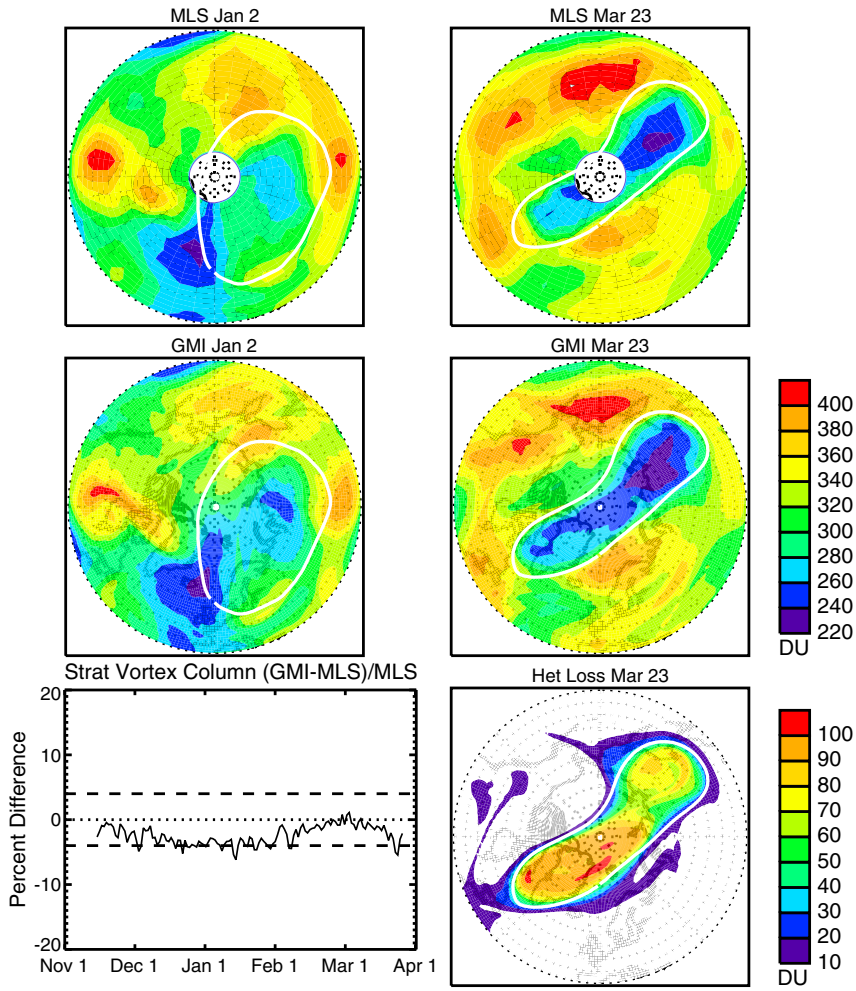

Figure 13. Top and middle rows: MLS and GMI stratospheric column O_3 on 2 January and 23 March 2011. White line indicates the vortex edge. Bottom left: Percentage difference between the daily vortex-averaged O_3 column simulated by GMI Het and MLS. The dashed lines indicate the 2σ uncertainty. Bottom right: PSC-driven O_3 loss determined by the column difference between GMI Het and No Het.

5. The Final Warming in April 2011

[33] The March Arctic and October Antarctic total column O_3 means are often used to illustrate interhemispheric differences in polar O_3 loss [*WMO*, 2011]. The Antarctic shows large decreases in O_3 since 1980 in the 40 year time series shown in Figures 2–8 of the *WMO Report* [2011], while the Arctic shows a smaller O_3 decline and large IA variability. The large IA variability of Arctic O_3 is driven by IA variability in planetary wave driving [*Chipperfield and Jones*, 1999; *Randel et al*., 2002] and in chemical loss. However, chemical loss is correlated with cold winters, which have intrinsically weaker transport and thus lower O_3 regardless of chemical loss [*Newman et al*., 2001]. The wave-driven residual circulation can transport 60–145 DU ozone to the Arctic between fall and spring, with lesser amounts transport during cold winters (<100 DU) and greater amounts in warm winters [*Tegtmeier et al*., 2008]. As Figure 2a shows that ~40 DU of that transport occurs before mid-January, this suggests that 20–60 DU O_3 may be transported to the Arctic in late winter. The breakdown of the vortex results in strong horizontal mixing with midlatitude air, increasing Arctic ozone. For example, data from 2005–2010 presented in Figure 1c show that Arctic mean O_3 typically increases from 350 to 400 DU between mid-January and the end of March. The March Arctic mean usually includes an O_3 transport contribution from the final warming, but occasionally the vortex remains intact and over the pole at the end of March. In such cases, the late winter transport contribution to high spring O_3 has not yet occurred, resulting in unusually low March Arctic column O_3 (e.g., 1997 [*Coy et al*., 1997]).

[34] Figures 1a and 1b show OMI and MLS column O_3 on 24 March 2011. The vortex is large and strong on this date. Columns inside the vortex are low in part due to chemical O_3 loss, but also because a significant fraction of the seasonal poleward transport of high O_3 has not yet occurred. Figure 14a shows total column O_3 measured by OMI on 10 April 2011. *Hurwitz et al*. [2011] report the 450 K vortex breakdown occurs on 10 or 19 April, depending on the meteorological analysis used. The vortex, with column O_3 of less than 300 DU, is pushed off the pole and replaced by midlatitude air with columns greater than 440 DU. Figure 14b shows time series of OMI daily column O_3 averaged over 63–90°N from 10 February to 1 May 2005–2011. Except for 2005 and 2011 (purple and red), Arctic daily column means are above 400 DU before the end of February. In 2005, the late winter transport of high O_3 occurs in mid-March (purple) as the vortex breaks down; this produces a mean March Arctic column for 2005 that is lower than the other years, not just because of chemical loss that took place, but because of the timing of the transport. The final warming in 2011 begins in early April, and the associated large O_3 transport is not part of the March average. By mid-April 2011, the OMI Arctic column O_3 is quite similar to the other years. The use of April instead of March mean Arctic O_3 would reduce much of the IA variability seen in Arctic O_3 in the past 30 years [e.g., *Tegtmeier et al*., 2008; *WMO*, 2011]; however, it would be difficult to assess O_3 losses because by April the ozone-depleted vortex air is usually dispersed into the midlatitudes. The situation in the Antarctic is quite different, where IA variability in the timing of chemical losses and the vortex breakdown rarely contribute to the October mean O_3. Chemical O_3 loss in Arctic cannot be accurately assessed without quantitative consideration of transport.

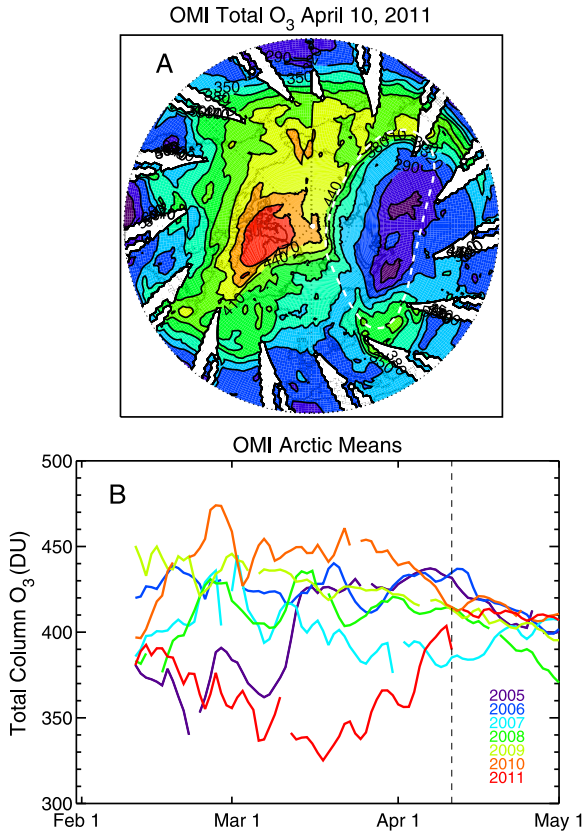

Figure 14. (a) OMI total column O_3 on 10 April 2011, as the final warming begins. (b) Daily OMI Arctic mean total column O_3 (63–90°N) for seven winter and spring seasons. OMI data are only shown after 10 February when observations first reach 70°N. In all years except 2005 and 2011, Arctic column O_3 is above 400 DU almost daily in February and March. The 2011 vortex broke down later than the other years shown, but mean columns exceeding 400 DU are reached by mid-April.

6. Discussion and Summary

[35] Low IA variability inside the Arctic vortex in early winter combined with the exceptionally weak polar transport in the winter of 2011 provide the basis for using Aura MLS O_3 and N_2O observations to separate the contributions of chemistry and transport to the low O_3 columns observed in March 2011. Mean March Arctic O_3 has large IA variability that complicates efforts to separate the effects of chemistry and transport. We show that Arctic O_3 variability comes from columns outside the vortex (outside PSC-forming regions), vortex area, and the timing of the final warming that transports high levels of O_3 poleward. Column O_3 inside the vortex shows little IA variability for the winters of 2005–2011 prior to the first warming of the season. These data allow us to estimate the amount of O_3 in the LS vortex column before large chemical losses began in early February. The analysis of vortex O_3 behavior presented here is made

possible by the continuous three-dimensional coverage of the polar region by the MLS instrument.

[36] We quantify the effects of chemistry and transport on vortex column O_3 by separately evaluating the behavior of the LS column, which is affected by heterogeneous chemistry and transport, and that of the LMS and MS columns, which are mainly affected by transport. In contrast to the behavior observed in 2005–2010, the MLS LMS and MS 2011 columns show a near total lack of transport into the vortex between late January and late March. We also quantify late winter O_3 transport in these columns using the GMI "No Het" simulation, obtaining results that agree well with the MLS calculation. In addition, we confirm that heterogeneous chemical loss in these partial columns was small by comparing GMI simulations with and without heterogeneous chemical reactions. The difference in vortex partial columns in these simulations showed 1 DU loss in the LMS and MS columns combined. The sum of these MLS vortex partial columns is 15–35 DU lower in late March than any of the previous 6 years. Contoured PDFs of MLS N_2O confirm the isolation of the LS vortex in 2011. With negligible meridional mixing into the vortex, we were able to use the descent of observed vortex N_2O profiles between late January and late March to estimate that vertical transport brought 12 ($\pm$7) DU O_3 into the LS vortex column during the period of PSC-driven chemical loss. The isolation of the vortex is critical for the calculation of the late winter contribution of descent to the LS column O_3; winters from 2004 to 2010 do not show sufficient isolation for this method.

[37] We separate the calculation of seasonal loss of stratospheric vortex column O_3 into early and late winter contributions. The GMI model results show 13 DU O_3 loss during December and January. This is consistent with our estimate of early season loss based on the small range of LS vortex O_3 observed (170–185 DU) and the shift of the 2010–2011 LS column from the high to the low side of the data envelope (Figure 6). During late winter (late January to late March), MLS data show a decrease in LS vortex column O_3 of 56 DU. Using the descent of N_2O profiles, we infer that descent provides a net contribution of 12 DU O_3, which includes a 2 DU gas phase loss due to $NO_2 + O$. Thus, the combined late winter LS O_3 heterogeneous loss is 68 DU. When we include the 1 DU loss in the LMS and MS calculated by the GMI model in late winter, the 2 DU loss in the LS that is transported to the LMS, and the early season loss of 13 DU, the total column vortex-averaged loss for the season is 84 ± 12 DU. The difference between the GMI Het and No Het simulations shows that 73 DU were lost by late March. The difference between the model result and the MLS-derived quantity comes from insufficient descent in the model LS vortex in late winter, which results in a 7–10 DU underestimate of O_3 transport and hence chemical loss. The GMI N_2O PDFs closely match those calculated using MLS N_2O, providing evidence that the model produces a realistically isolated vortex and supporting the use of the GMI simulations to calculate O_3 loss.

[38] We estimate that the vortex mean stratospheric column in late March in the absence of heterogeneous chemistry would have been 365 DU. This "no loss" Arctic column is very similar to pre-ozone hole total columns observed in the Antarctic by the Nimbus 4 BUV in 1970–1972 [*Stolarski et al*., 1997; *WMO*, 2011]: 353–372 DU. This underscores the meteorological similarity between the 2011 Arctic vortex and the Antarctic.

[39] The observed vortex-averaged stratospheric column for late March is 281 DU (Figure 12). This represents a PSC-driven loss of 84 (12) DU averaged over the vortex, somewhat higher than the 65 DU calculated in a CTM simulation [*Balis et al*., 2011]. *Adams et al*. [2012] and *Lindenmaier et al*. [2012] both used an offline chemistry transport model simulation (SLIMCAT) carrying passive O_3 (no chemistry) and reported losses of 99–108 DU between 12 and 20 March. *Sinnhuber et al*. [2011] report vortex losses of more than 140 DU by early April based on model calculations with a passive O_3 tracer. Their simulated vortex N_2O, initialized with MIPAS data on 1 December, was 40 ppb too high compared to MIPAS by mid-February at 475 K. This indicates either insufficient descent, or sufficient descent but without vortex isolation. None of these studies demonstrated the isolation of their simulated vortex. In the lower stratosphere where O_3 is higher outside the vortex (due to O_3 loss in the vortex), mixing across the vortex edge can transport significant O_3 amounts into the vortex, allowing the vortex to function as a "flowing processor", resulting in increased estimates of O_3 loss. Problems with vortex isolation also affect simulated O_3 chemistry by way of vortex Cl_y (and thus ClO_x), which will be too low when the vortex edge is inadequately represented [*Waugh et al*., 2007; *SPARC*, 2010]. The contoured MLS N_2O PDFs clearly rule out the influx of high O_3 midlatitude air into the LS vortex in late winter 2011. By showing the same features, the GMI N_2O PDFs similarly indicate that such an influx does not occur in the simulation either.

[40] Vortex ozone deficits of greater than 130 DU are shown in Figure 5d of *Manney et al*. [2011]. The deficit was calculated by subtracting the 2011 OMI O_3 data from daily Arctic column O_3 observations averaged over 1979–2010, a period they choose as having minimal chemical ozone loss. This 32 year mean O_3 implicitly reflects the Arctic climatological mean meteorology, which includes the final warming occurring by late March. The final warming in 2011, which occurred in April, contributes 40 DU or more to the Arctic mean. The *Manney et al*. [2011] supplement recognizes the importance of O_3 resupply, both by descent and horizontal mixing into the vortex, to the spring column. Although they do not quantify transport, they note that both processes were very weak in 2011. Weak transport processes resulting from the unusual dynamics of the 2011 vortex explain the difference between the >130 DU ozone deficit shown in *Manney et al*. [2011] and the >90 DU chemical ozone loss contour in Figure 13.

[41] The final warming that resupplies O_3 to high latitudes is an essential component of seasonal transport in the Arctic, and resupply is not complete—or even begun—in some years by the end of March (e.g., 1997 and 2011). OMI data have excellent coverage of the Arctic in March and April, demonstrating that long-lasting low temperatures were not the only unusual feature of the 2011 Arctic stratosphere. A long-lasting vortex means a late resupply, which in 2011 began well after 1 April. Heterogeneous chemical O_3 loss in the Arctic was large in 2011, 84 DU averaged over the vortex, but the timing of the final warming is also an

important part of the story. The 2011 Arctic O_3 loss may be the largest ever observed, but it is still considerably less than the 120–150 DU range of Antarctic losses reported by *Tilmes et al*. [2006].

[42] **Acknowledgments.** We thank the diligent efforts of the reviewers whose comments and suggestions substantially strengthened this paper. We thank Stephen Steenrod for running the GMI CTM simulations. This work was supported by the NASA Modeling, Analysis, and Prediction Program and the NASA Atmospheric Composition Modeling and Analysis Program.

References

Adams, C., et al. (2012), Severe 2011 ozone depletion assessed with 11 years of ozone, NO_2, and OClO measurements at 80°N, *Geophys. Res. Lett.*, *39*, L05806, doi:10.1029/2011GL050478.

Allen, D. R., A. R. Douglass, G. L. Manney, S. E. Strahan, J. C. Krosschell, J. V. Trueblood, J. E. Nielsen, S. Pawson, and Z. Zhu (2011), Modeling the frozen-in anticyclone in the 2005 Arctic summer stratosphere, *Atmos. Chem. Phys.*, *11*, 4557–4576.

Anton, M., M. López, J. M. Vilaplana, M. Kroon, R. McPeters, M. Bañón, and A. Serrano (2009), Validation of OMI-TOMS and OMI-DOAS total column ozone using five Brewer spectroradiometers at the Iberian peninsula, *J. Geophys. Res.*, *114*, D14307, doi:10.1029/2009JD012003.

Balis, D., et al. (2011), Observed and modeled record ozone decline over the Arctic during winter/spring 2011, *Geophys. Res. Lett.*, *38*, doi:10.1029/2011GL049259.

Chipperfield, M. P., and R. L. Jones (1999), Relative influences of atmospheric chemistry and transport on Arctic ozone trends, *Nature*, *400*, 551–554.

Considine, D. B., A. R. Douglass, P. S. Connell, D. E. Kinnison, and D. A. Rotman (2000), A polar stratospheric cloud parameterization for the global modeling initiative three-dimensional model and its response to stratospheric aircraft, *J. Geophys. Res.*, *105*, 3955–3973.

Coy, L., E. R. Nash, and P. A. Newman (1997), Meteorology of the polar vortex: Spring 1997, *Geophys. Res. Lett.*, *24*, 2693–2696.

Douglass, A. R., and S. R. Kawa (1999), Contrast between 1992 and 1997 high-latitude spring Halogen Occultation Experiment observations of lower stratospheric HCl, *J. Geophys. Res.*, *104*, 18,739–18,754.

Duncan, B. N., S. E. Strahan, Y. Yoshida, S. D. Steenrod, and N. Livesey (2007), Model study of cross-tropopause transport of biomass burning pollution, *Atmos. Chem. Phys.*, *7*, 3713–3736.

Hood, L., B. Soukharev, M. Fromm, and J. McCormack (2001), Origin of extreme ozone minima at middle to high northern latitudes, *J. Geophys. Res.*, *106*, D18, doi:10.1029/2001JD900093.

Hurwitz, M. M., P. A. Newman, and C. I. Garfinkel (2011), The Arctic vortex in March 2011: A dynamical perspective, *Atmos. Chem. Phys*, *11*, 11,447–11,453.

Kawa, S. R., R. M. Bevilacqua, J. J. Margitan, A. R. Douglass, M. R. Schoeberl, K. W. Hoppel, and B. Sen (2002), Interaction between dynamics and chemistry of ozone in the setup phase of the Northern Hemisphere polar vortex, *J. Geophys. Res.*, *107*, 8310, doi:10.1029/2001JD001527.

Lindenmaier, R., et al. (2012), Unusually low ozone, HCl, and HNO_3 column measurements at Eureka, Canada during winter/spring 2011, *Atmos. Chem. Phys.*, *12*, 3821–3835.

Livesey, N., et al. (2011), Earth Observing System (EOS) Aura Microwave Limb Sounder (MLS) Version 3.3 Level 2 data quality and description document, JPL D-33509.

Manney, G. L., et al. (2011), Unprecedented Arctic ozone loss in 2011, *Nature*, *478*, 469–475, doi:10.1038/nature10556.

Müller, R., P. J. Crutzen, J.-U. Grooß, C. Bruehl, J. M. Russell III, and A. F. Tuck (1996), Chlorine activation and ozone depletion in the Arctic vortex: Observations by the Halogen Occultation Experiment on the Upper Atmosphere Research Satellite, *J. Geophys. Res.*, *101*, 12,531–12,554.

Müller, R., J.-U. Grooß, C. Lemmen, D. Heinze, M. Dameris, and G. Bodeker (2008), Simple measures of ozone depletion in the polar stratosphere, *Atmos. Chem. Phys.*, *8*, 251–264.

Müller, R. M., S. Tilmes, P. Konopka, J.-U. Grooß, and H.-J. Jost (2005), Impact of mixing and chemical change on ozone-tracer relations in the polar vortex, *Atmos. Chem. Phys.*, *5*, 3139–3151.

Nash, E. R., P. A. Newman, J. E. Rosenfield, and M. R. Schoeberl (1996), An objective determination of the polar vortex using Ertel's potential vorticity, *J. Geophys. Res.*, *101*, 9471–9478.

Newman, P. A., E. R. Nash, and J. E. Rosenfield (2001), What controls the temperature of the Arctic stratosphere during the spring?, *J. Geophys. Res.*, *106*, D17, doi:10.1029/2000JD000061.

Randel, W. J., F. Wu, and R. Stolarski (2002), Changes in column ozone correlated with the stratospheric EP flux, *J. Met. Soc. Jap.*, *80*, 849–862.

Rex, M., R. J. Salawitch, P. von der Gathen, N. R. Harris, M. P. Chipperfield, and B. Naujokat (2004), Arctic ozone loss and climate change, *Geophys. Res. Lett.*, *31*, L04116, doi:10.1029/2003GL018844.

Rex, M., et al. (2006), Arctic winter 2005: Implications for stratospheric ozone loss and climate change, *Geophys. Res. Lett.*, *33*, L23808, doi:10.1029/2006GL026731.

Rienecker, M. M., et al. (2011), MERRA: NASA's Modern Era Retrospective Analysis for Research and Applications, *J. Climate*, *24*, 3624–3648.

Rosenfield, J., P. Newman, and M. Schoeberl (1994), Computations of diabatic descent in the stratospheric polar vortex, *J. Geophys. Res.*, *99*, doi:10.1029/94JD01156.

Sinnhuber, B.-M., G. Stiller, R. Ruhnke, T. von Clarmann, and S. Kellman (2011), Arctic winter 2010/2011 at the brink of an ozone hole, *Geophys. Res. Lett.*, *38*, doi:10.1029/2011/GL049784.

SPARC CCMVal (2010), *SPARC Report on the Evaluation of Chemistry-Climate Models*, V. Eyring, T. G. Shepherd, D. W. Waugh (Eds.), SPARC Report No. 5, WCRP-132, WMO/TD-No. 1526, http://www.atmosp.physics.utoronto.ca/SPARC.

Steinbrecht, W., H. Claude, U. Koehler, and K. P. Hoinka (1998), Correlations between tropopause height and total ozone: Implications for long-term changes, *J. Geophys. Res.*, *103*, 19,183–19,192.

Stolarski, R. S., G. J. Labow, and R. D. McPeters (1997), Springtime Antarctic total ozone measurements in the early 1970s from the BUV instrument on Nimbus 4, *Geophys. Res. Lett.*, *24*, 591–594.

Strahan, S. E., B. N. Duncan, and P. Hoor (2007), Observationally derived transport diagnostics for the lowermost stratosphere and their application to the GMI chemistry and transport model (2007), *Atmos. Chem. Phys.*, *7*, 2435–2445.

Tegtmeier, S., M. Rex, I. Wohltmann, and K. Krueger (2008), Relative importance of dynamical and chemical contributions to Arctic wintertime ozone, *Geophys. Res. Lett.*, *35*, L17801, doi:10.1029/2008GL034250.

Tilmes, S., R. Müller, A. Engel, M. Rex, and J. M. Russell III (2006), Chemical ozone loss in the Arctic and Antarctic stratosphere between 1992 and 2005, *Geophys. Res. Lett.*, *33*, L20812, doi:10.1029/2006GL026925.

Tilmes, S., R. Müller, J.-U. Grooß, D. S. McKenna, J. M. Russell III, and Y. Sasano (2003), Calculation of chemical ozone loss in the Arctic winter 1996–1997 using ozone-tracer correlations: Comparison of Improved Limb Atmospheric Spectrometer (ILAS) and Halogen Occultation Experiment (HALOE) results, *J. Geophys. Res.*, *108*, doi:10.1029/2002JD002213.

Waugh, D. W., S. E. Strahan, and P. A. Newman (2007), Sensitivity of stratospheric inorganic chlorine to differences in transport, *Atmos. Chem. Phys.*, *7*, 4935–4941.

WMO (World Meteorological Organization) (2011), Scientific assessment of ozone depletion: 2010, Global Ozone Research and Monitoring Project – Report No. 52, 516 pp., Geneva, Switzerland.